Effects of Hydrophobicity and Anions on Self-Assembly of the Peptide EMK16-II

Dawei Zou,[1] Zuoxiu Tie,[1] Chunmei Lu,[1] Meng Qin,[1] Xiaomei Lu,[1] Mu Wang,[1] Wei Wang,[1] P. Chen[2]

[1] *National Laboratory of Solid State Microstructure and Department of Physics, Nanjing University, Nanjing 210093, China*

[2] *Department of Chemical Engineering, University of Waterloo, 200 University Avenue West, Waterloo, Ontario N2L 3G1, Canada*

Received 30 July 2009; revised 18 September 2009; accepted 26 October 2009
Published online 2 November 2009 in Wiley InterScience (www.interscience.wiley.com). DOI 10.1002/bip.21340

ABSTRACT:

Effects of hydrophobic and electrostatic interactions on the self-assembling process of the ionic-complementary peptide EMK16-II are investigated by atomic force microscopy imaging, circular dichroism spectra, light scattering, and chromatography. It is found that the hydrophobicity of the peptide promotes the aggregation in pure water even at a very low concentration, resulting in a much lower critical aggregation concentration than that of another peptide, EAK16-II. The effect of anions in solution with different valences on electrostatic interactions is also important. Monovalent anions (Cl^- and Ac^-) with a proper concentration can facilitate the formation of peptide fibrils, with Cl^- of smaller size being more effective than Ac^- of larger size. However, only small amounts of fibrils, but plenty of large amorphous aggregates, are found when the peptide solution is incubated with multivalent anions, such as SO_4^{2-}, $C_6H_5O_7^{3-}$, and HPO_4^{2-}. More importantly, by gel filtration chromatography, the citrate anion, which induces a similar effect on the self-assembling process of EMK16-II as that of SO_4^{2-} and HPO_4^{2-}, can interact with two or more positively charged residues of the peptide and reside in the amorphous aggregates. This implies a "salt bridge" effect of multivalent anions on the peptide self-assembling process, which can interpret a previous puzzle why divalent cations inhibit the formation of ordered nanofibrils of the ionic-complementary peptides. Thus, our results clarify the important effects of hydrophobic and electrostatic interactions on the self-assembling process of the ionic-complementary peptides. These are greatly helpful for us to understand the mechanism of peptides' self-assembling process and protein folding and aggregation. © *2009 Wiley Periodicals, Inc. Biopolymers 93: 318–329, 2010.*

Keywords: *EMK16-II; ionic-complementary peptide; fibril aggregation; salt bridge*

Correspondence to: Meng Qin; e-mail: qinmeng@nju.edu.cn or Wei Wang; e-mail: wangwei@nju.edu.cn
Contract grant sponsor: National Natural Science Foundation of China
Contract grant number: 10834002
Contract grant sponsors: National Basic Research Program of China
Contract grant numbers: 2006CB910302 and 2007CB814800
©2009 Wiley Periodicals, Inc.

This article was originally published online as an accepted preprint. The "Published Online" date corresponds to the preprint version. You can request a copy of the preprint by emailing the Biopolymers editorial office at biopolymers@wiley.com

INTRODUCTION

Many human diseases, including many neurodegenerative disorders and amyloidoses, exhibit the accumulation of stable, ordered, and filamentous protein–peptide aggregates that are known as amyloid fibrils.[1–6] A common feature of these conformational diseases is that the related proteins or protein fragments can easily change from their soluble and functional forms into insoluble β-sheet-rich fibrils. These fibrils usually

deposit in a variety of organs and tissues. Previous experimental results exhibited that hydrophobicity, electrostatic interaction, and hydrogen bonds are the key factors for the aggregation, especially for the amyloid fibrils formed by the protein–peptide sequences containing special repeated residues. However, the mechanism of the aggregation is still not fully understood because of the complexity of these interactions. To make a detailed description of the aggregation process, recent studies have focused on investigating the self-assembly process of artificially synthesized peptides designed with repeated residues or the aggregate-causing fragments of the protein.[7–9] In fact, the self-assembled aggregates of the peptides have also been found to have potential applications in biomedicine, such as tissue repair,[10–12] drug delivery,[13,14] and biological surface engineering.[15–17]

The most popular self-assembling oligopeptides investigated in recent years are the ionic-complementary EAK16 family. They are originally found in a left-handed Z-DNA-binding protein named zuotin in yeast and have many potential applications.[18,19] This type of peptide (i.e., EAK16-II) contains a repetitive charge distribution and alternating hydrophobic and hydrophilic residues in the amino acid sequence. They are short, simple to design, extremely easy to synthesize, and well investigated by numerous studies in recent years.[18,20–22] In particular, they can form unusually stable β-sheet structure and aggregate to become fibrils or other nanostructures with different applications mainly because of the electrostatic interactions.[7,9,23–28] Previous studies indicate that the self-assembling process involves almost all the interactions, i.e., the hydrogen bonds, hydrophobic, and electrostatic interactions, dominated in the formation of amyloid fibrils of proteins.[22,29,30] However, these interactions, which are determinants in the peptide self-assembling,[29] can be easily affected by adjusting the solution conditions, such as pH, ions, and so on,[7,9,26] because charged amino acids play an important role in determining the stable conformation of a peptide through electrostatic interaction and hydrogen bonding. These features can help us to understand the mechanism of peptide self-assembly.

It is known that the pH of the peptide solution can affect the ionic state of the charged amino acids, which further influences the formation of the secondary structures of the peptide,[31,32] even the aggregates or the macroscopic nanofibers.[7,33] The self-assembling process can also be influenced by the concentration of salts, valences of the cations and anions dissolved in the peptide solution, or even different types of ions with the same valence.[34] In a typical surfactant solution, monovalent salts can screen the charge interactions[27] between the polar groups of the molecule and reduce the electrostatic repulsion, resulting in a decrease in the critical micelle concentration[9] and the formation of more ordered morphology of self-assembling nanostructures.[35] However, divalent ions, instead of inducing the ordered structure or membrane formation, contribute to the formation of disordered aggregation of the peptide.[18] There is an exception observed by Chen and coworkers[26] that Cu^{2+} can bind the imidazole of histidine to facilitate the fibril formation of the peptide EAK16II-GGH. Our sample EMK16-II is quite different from EAK16II-GGH because there is no specific tail in our peptide. However, it is still unknown why multivalent ions are ineffective to the formation of fibrils or membranes. In fact, although the sequential and structural features of synthesized ionic-complementary peptides are much more simple than the corresponding proteins involved in amyloid fibrils, the mechanism of the formation of diverse types of peptides' self-assembling fibrils is still unclear.[19] Thus, understanding of the different effects of the hydrophobicity, electrostatic interaction, and hydrogen bonds in the self-assembling process will be greatly helpful for us to study the self-assembling processes of peptides and related proteins.

In this work, we design and synthesize the ionic-complementary peptide EMK16-II[36] using the same sequencing rule as for EAK16-II[22] by substituting alanine (Ala, A) in EAK16-II with methionine (Met, M). The reason for using methionine is that it is more hydrophobic than alanine and is relatively simple with a straight side chain comparing with other more hydrophobic residues, e.g., leucine and so on. Through investigating the self-assembling process, this newly synthesized peptide has similar interactions as the former one (EAK16-II), but stronger hydrophobicity yields a much lower critical aggregation concentration (CAC) than EAK16-II[25] even when the C- and N-terminus are free without protection groups.[37] To describe the effect of the electrostatic interactions on peptide self-assembling properties, the solution environment of the charged residues is modulated by adding different anions with different valences and by adjusting the solution pH conditions from pH 4.5 to 9.0. The self-assembling process is studied by using techniques of atomic force microscopy (AFM) imaging, circular dichroism (CD) spectrum, light scattering (LS), dynamic LS (DLS), and chromatography. It will be shown that monovalent anions (i.e., Cl^- and Ac^-) at proper concentrations can facilitate the formation of fibrils by screening the net charges of peptide, which corresponds well with previous studies.[35,38] In addition, even for a single monovalent anion, the morphology of fibrils can also be affected by adjusting pH of the solutions.

As will be shown, only small amounts of fibrils but plenty of large amorphous aggregates are observed in the self-assembling process when the peptide solution is incubated with multivalent anions, such as SO_4^{2-}, $C_6H_5O_7^{3-}$, and HPO_4^{2-}. For the case of one of these typical salts with multi-

10970282, 2010, 4, Downloaded from https://onlinelibrary.wiley.com/doi/10.1002/bip.21340 by Universidade do Porto, Wiley Online Library on [02/12/2025]. See the Terms and Conditions (https://onlinelibrary.wiley.com/terms-and-conditions) on Wiley Online Library for rules of use; OA articles are governed by the applicable Creative Commons License

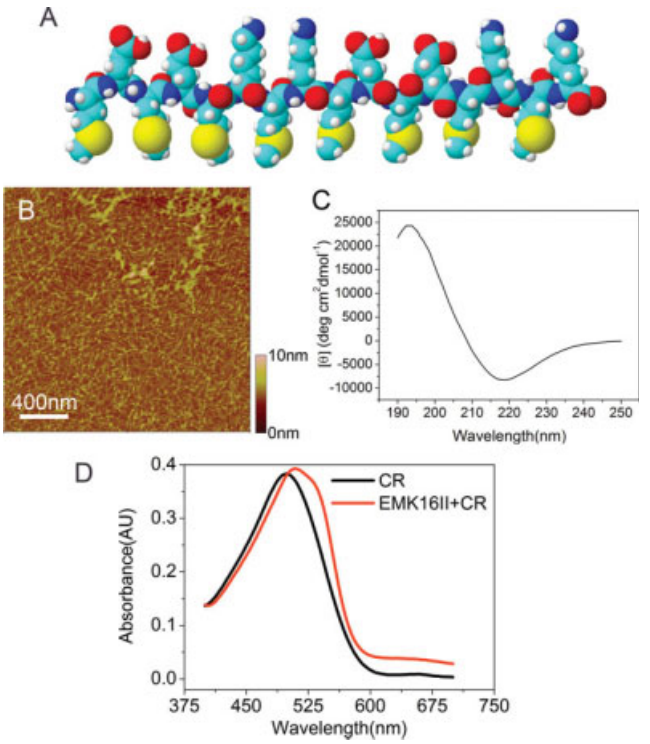

FIGURE 1 (A) Schematic molecular model of EMK16-II. The sequence is MEMEMKMKMEMEMKMK, where carbon atoms are cyan, oxygen atoms are red, nitrogen atoms are blue, sulfur atoms are yellow, and hydrogen atoms are white. In this conformation, the hydrophobic methionine side chains reside in one side and the lysine and glutamic acid side chains reside in the other side. (B) AFM image of self-assembling nanofibrils of EMK16-II in pure water. (C) The far-UV CD spectrum of EMK16-II at room temperature. (D) Shift of the Congo red absorption peak after adding EMK16-II. Absorbance spectra of unbound Congo red (black line) and Congo red bound to 0.4 mg/ml EMK16-II in water (red line).

valent anions, phosphate buffer was investigated in our previous study[36] to describe the effect of concentrations of the multivalent anions on the self-assembling process of EMK16-II. In Ref. 36, it was found that the ordered fibrils are gradually destroyed to form amorphous aggregates by increasing the concentration of multivalent anions because of the proposed effect of "salt bridge." By comparing this work with our previous one, we not only largely extend the study content to five different multivalent anions but also consider the effect of pH conditions. Most importantly, as the typical multivalent anions, the citrate anions with high UV-absorption were found by gel filtration chromatography to interact with two or more positively charged groups as "bridges" and reside stably inside the amorphous aggregates. The effect of multivalent anions on the self-assembling process is defined as the "salt bridge" effect. Such an effect of salt bridge can clearly elucidate the puzzle why divalent cations are the inhibitors for the formation of the ordered fibrils of the ionic-complimentary peptides as discussed in previous studies.[9,26,39,40] These results show the importance of the effects of the hydrophobic and electrostatic interactions on the self-assembling process of the ionic-complimentary peptides.

RESULTS AND DISCUSSION

Figure 1A shows the three-dimensional structure of EMK16-II using the ChemSketch software based on energy minimization.[41] Hydrophilic residues (Glu and Lys) are located on one side of EMK16-II, and hydrophobic residues (Met) are located on the opposite side, exhibiting amphiphilic feature with two distinct hydrophilic and hydrophobic interfaces. At neutral pH, Glu and Lys are negatively and positively charged, respectively (Met is a neutral residue), therefore, the charge sequence of EMK16-II is: $- - + + - - + +$. From the AFM image shown in Figure 1B, EMK16-II forms well-ordered peptide fibrils in pure water. The width and height of these fibrils are 16.1 $\pm$ 1.7 and 1.4 $\pm$ 0.1 nm, respectively, indicating that EMK16-II tends to adopt a double-layer structure like RADA16[42] and EAK16-II.[43] Especially, the height of fibrils does not change with the increase or decrease of the concentrations of the peptide, which is different from that of EAK16-II.[25] It is proposed that the formation of the double-layer fibrils is mainly driven by the stronger hydrophobicity. As shown in Figure 1C, two special peaks, one minimum at 218 nm and one maximum at 195 nm, symbolize the typical β-sheet structure. At the same time, the β-sheet content is calculated to be about 96%.[44,45] In addition, the existence of these amyloid-like fibrils can be further confirmed by Congo red assay[46] as shown in Figure 1D. It is noted that the red shift of the absorption occurs only in a few minutes after the peptide dissolution, which indicates that the kinetic formation process of fibrils is extremely fast. This demonstrates that the peptide can easily self-assemble into β-sheet-rich amyloid fibril-like structures in pure water.

The CAC is a general parameter to describe the self-assembling features of peptides in many studies.[25,26,47] Figure 2A shows that the intensity of LS is dependent on concentrations of the peptide (from 0.005 to 0.5 mg/ml). There is no increase in LS intensity in the low concentration range (0.005–0.02 mg/ml), indicating that no aggregation occurs at such low concentrations. However, the LS intensity increases rapidly with time when the concentrations increase up to 0.05 mg/ml. As described by Fung et al.,[25] the changing rate of LS intensity, which can be related to the aggregation rate, is very different for the concentration below and above the CAC. It is shown in Figure 2B that there is a rapid transition of the slope between 0.02 and 0.05 mg/ml, which corre-

10970282, 2010, 4, Downloaded from https://onlinelibrary.wiley.com/doi/10.1002/bip.21340 by Universidade do Porto, Wiley Online Library on [02/12/2025]. See the Terms and Conditions (https://onlinelibrary.wiley.com/terms-and-conditions) on Wiley Online Library for rules of use; OA articles are governed by the applicable Creative Commons License

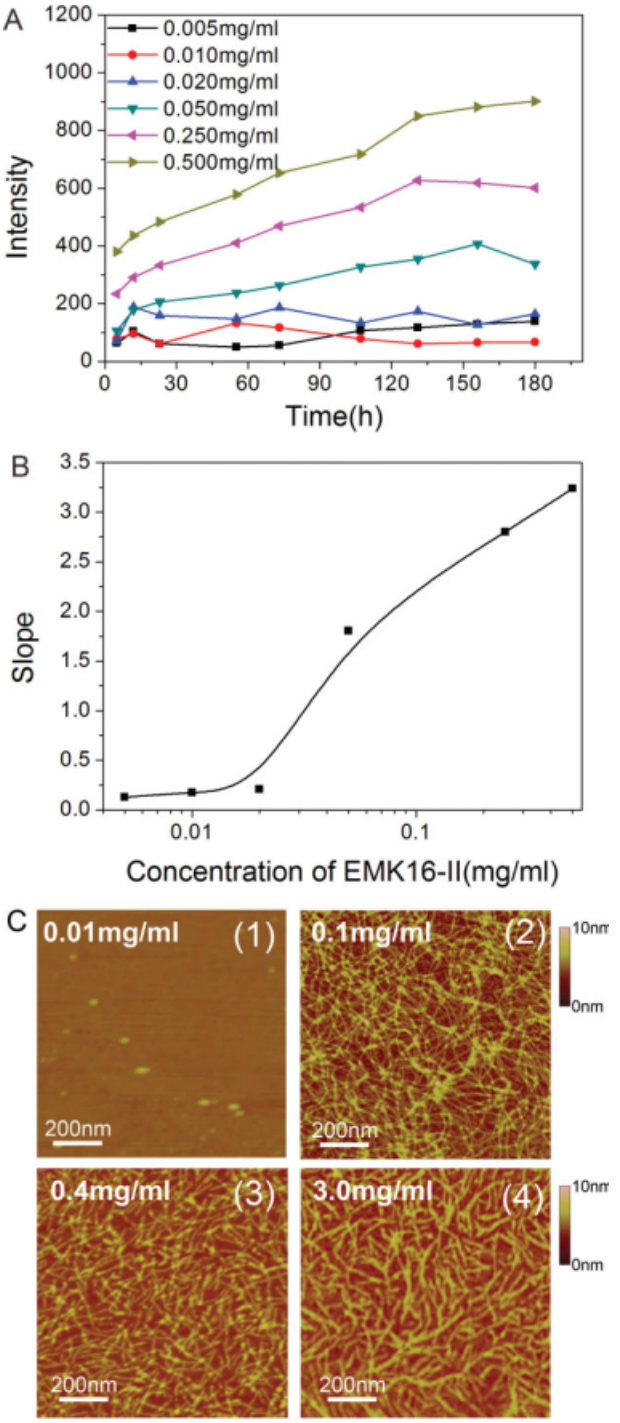

FIGURE 2 (A) Light scattering (LS) intensity of EMK16-II solutions changes with time at different concentrations from 0.005 to 0.5 mg/ml. In the conditions of high concentrations (0.05–0.5 mg/ml), the LS intensity increases rapidly as time passes. However, the LS intensity does not change with time in the conditions of low concentrations (0.005–0.02 mg/ml). (B) The rate of LS intensity changes over the first 100 h (slope obtained from Figure 2A) as a function of concentration. The value increases dramatically from 0.21 to 1.88 around the CAC, and two groups of data are obviously separated. (C) AFM images of the self-assembling nanofibrils of EMK16-II at different concentrations in pure water.

sponds to the region of CAC. As a result, the CAC of EMK16-II is below 0.05 mg/ml, which is about half as EAK16-II[25] (CAC is 0.1 mg/ml) because of the stronger hydrophobicity of residue Met. The different concentration of EMK16-II is also considered as show in Figure 2C. When the concentration of peptide is larger than CAC, the higher concentration of EMK16-II leads to wider fibrils, which accords well with the change of LS intensity (Figure 2A). In addition, when the concentration is lower than CAC, no fibrillar aggregates are observed as shown in Figure 2C (1).

As mentioned above, the electrostatic interaction is one of the dominant forces in protein folding and aggregation as well as peptide self-assembly.[23] The assembling features of peptides (or aggregation of proteins) can be modulated by ions. To investigate the effects of ions on the self-assembling process, five kinds of sodium salts with anions of different valences are taken in this study. In addition, for each salt solution, both the anionic valences and the electrostatic interaction are controlled by adjusting the pH value of the solution.

As a kind of typical monovalent salt, sodium chloride has been intensively used in many studies to explore its effects on the formation of amyloid fibrils of proteins and the self-assembling process of peptides.[27,35,37–39] As shown in Figures 3A–3C, EMK16-II self-assembles into typical ribbon-like nanofibers in solutions (containing 0.4 mg/ml EMK16-II and 20 m*M* NaCl) under different pH conditions with pH 4.5, 6.5, and 9.0, respectively. In fact, it is found in previous studies that the aggregation of the peptides strongly depends on the conditions of solution. Thomson and coworkers[48] observed that only short fibrils are formed at pH 3.6 in 0.4*M* NaCl and much longer fibrils at pH 2.5 at low ionic strengths (<30 m*M*). Similar results are also obtained by de la Paz et al.[37] Here, the relative low concentration of NaCl is applied to investigate its promoting effect on the self-assembling process of peptide EMK16-II. In addition, the same concentration is also applied to the multivalent anionic salts to compare the effects induced mainly by the different valences of anions. In addition, the CD spectra (shown in Figure 4) of EMK16-II in sodium chloride at three pH conditions show clearly that there is a specific negative peak at 218 nm and a positive peak at 195 nm, fully consistent with the typical features of β-sheet structure.

The dimensions of the EMK16-II nanofibrils shown in Figure 3 are summarized in Table I. The length of the nanofibrils (Figure 3B, 880.9 ± 52.0 nm) formed in 20 m*M* NaCl solutions at pH 6.5 is much longer than that in pure water (Figure 1B, 468.0 ± 24.0 nm). This indicates that proper concentration of NaCl promotes the formation of the ordered self-assembling nanostructure based on the β-sheet

10970282, 2010, 4, Downloaded from https://onlinelibrary.wiley.com/doi/10.1002/bip.21340 by Universidade do Porto, Wiley Online Library on [02/12/2025]. See the Terms and Conditions (https://onlinelibrary.wiley.com/terms-and-conditions) on Wiley Online Library for rules of use; OA articles are governed by the applicable Creative Commons License

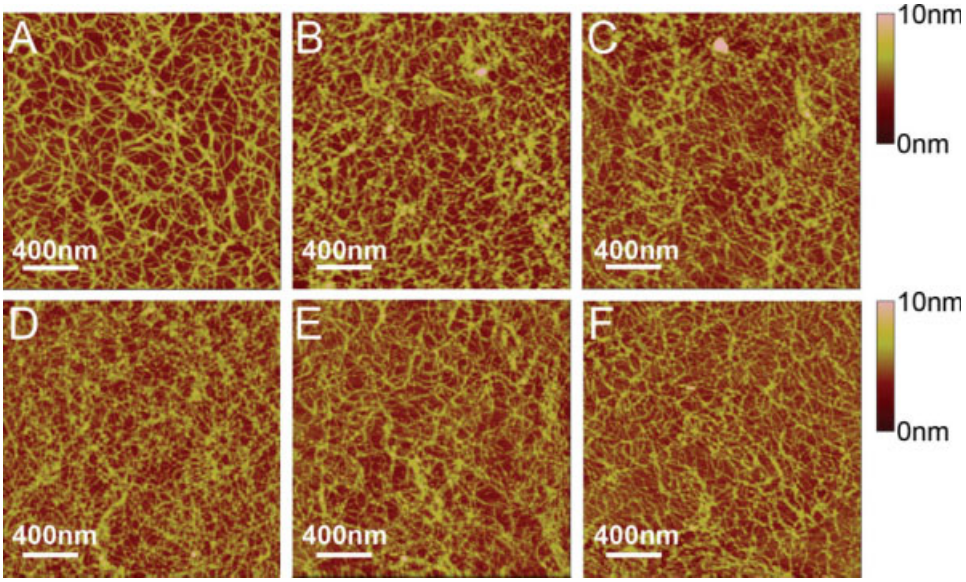

FIGURE 3 AFM images of the self-assembling nanofibrils of EMK16-II (0.4 mg/ml) in solutions containing 20 m*M* sodium chloride buffer at (A) pH 4.5, (B) pH 6.5, and (C) pH 9.0 and sodium acetate buffer at (D) pH 4.5, (E) pH 6.5, and (F) pH 9.0.

between the peptide molecules as observed in previous studies relating to EAK16-II[35] and coiled coil.[38] It is further confirmed by the CD spectra (the curve of pH 6.5 in Figure 4B) that the negative peak at 218 nm in NaCl solution is obviously lower than that in pure water. These results are mainly induced by the presence of the monovalent salts, which can screen the charged residues and further reduce the intermolecular electrostatic repulsion. The screening effect makes the charged residues be more hydrophobic[27] and further promotes the fibril elongation[35] by making the hydrogen bonding interaction between the adjacent peptides be more ordered. Moreover, as shown in Table I, there is no significant difference in widths and heights of these nanofibrils in NaCl solution under different pH conditions, which perhaps is due to the increased hydrophobicity in keeping the fibrils more stable in their width and height.

In addition, the differences in the lengths of fibrils at different pHs can be obtained from Table I. It is known that the p*K*a values of the side chains of glutamic acid and lysine are 4.25 and 10.53, respectively. We select pH 4.5 next to the p*K*a value of glutamic acid and pH 9.0 near the p*K*a value of lysine, so that either glutamic acid or lysine is partially neutralized. At non-neutral pHs (pH 4.5 and 9.0), the lengths of nanofibrils in solutions with pH 4.5 and 9.0 are a little shorter than that under the neutral pH condition likely due to the effect of electrostatic repulsion because there are net charges existing on the peptide because of the incomplete deprotonation and protonation of the side chains of Glu and Lys, respectively.

As a weak electrolyte, sodium acetate (20 m*M*, p*K*a 4.76) is another monovalent salt used in this work and is completely ionized both at neutral (pH 6.5) and at basic (pH 9.0) conditions. Even at pH 4.5, the Ac^-concentration is about 7 m*M* because of the hydrolysis of Ac^-, which is still over excessive to the concentration of the peptide (0.19 m*M*). Therefore, the differences of Ac^- concentrations under different pH conditions could be neglected. As shown in Figures 3D–3F, there is no obvious changes in the widths and heights of fibrils in NaAc solutions, as well as in water. However, the length of the fibrils is a little longer in neutral condition than that in water. The reason is similar to that in NaCl solution as discussed above. In addition, the CD spectra (Figure 4) clearly show the specific negative peak at 218 nm and positive peak at 195 nm, fully consistent with that of the β-sheet structure. However, the value of negative peak is lower than that in pure water, indicating that NaAc can also promote the formation of the nanofibrils like NaCl does. From Table I, it is also found that the length of fibrils in NaAc solution is shorter than that in NaCl solution. Because the molecular weight and volume of the Ac^- are much bigger than those of the Cl^-, the screening effect of Ac^- on the peptide is less obvious than that of the Cl^-. As discussed above, EMK16-II carries net positive charges in solutions at pH 4.5, net negative charges in solutions at pH 9.0, and no net charges in neutral solutions. Comparing with the neutral situation, more Ac^- anions in solution at pH 4.5 can interact with the peptide bringing steric effect more prominent, which induces

10970282, 2010, 4, Downloaded from https://onlinelibrary.wiley.com/doi/10.1002/bip.21340 by Universidade do Porto, Wiley Online Library on [02/12/2025]. See the Terms and Conditions (https://onlinelibrary.wiley.com/terms-and-conditions) on Wiley Online Library for rules of use; OA articles are governed by the applicable Creative Commons License

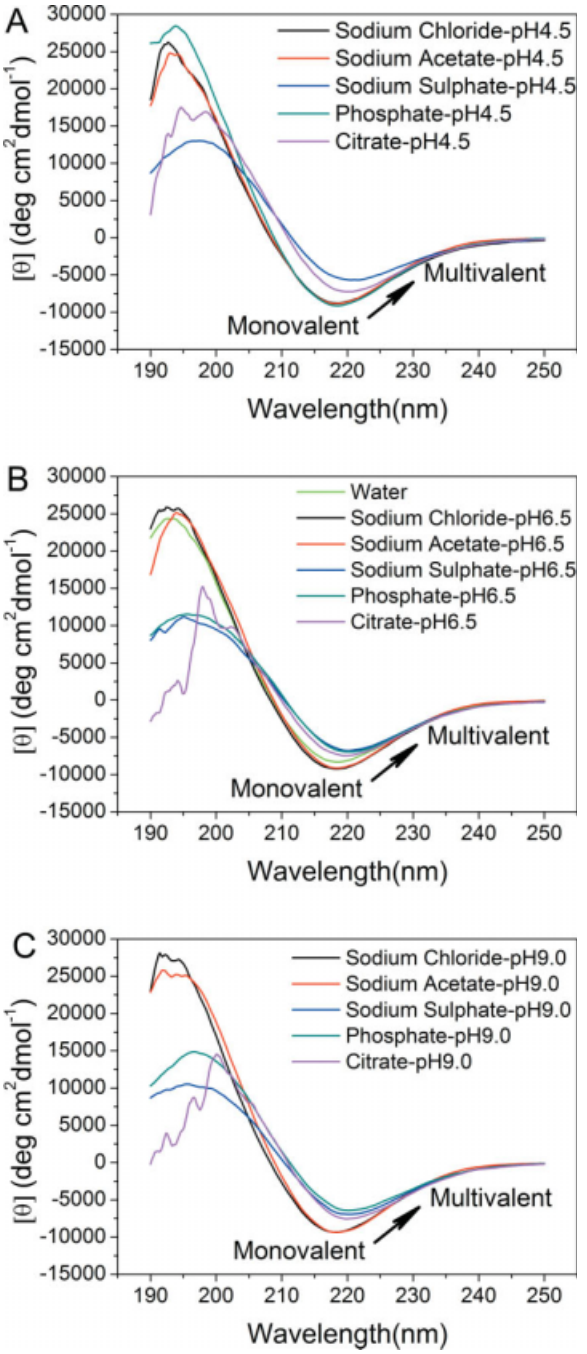

FIGURE 4 Far-UV CD spectra of 0.4 mg/ml EMK16-II in pure water and different buffers at three pHs: (A) pH 4.5, (B) pH 6.5, and (C) pH 9.0. Under each pH condition, the position and amplitude of the negative peaks show changes according to the different valences of anions in solutions. In addition, multivalent anions can lead to the diminishment and red shift of the negative band at 218 nm, which represents the decrease of the β-sheet structure.

the formation of shorter fibrils. In contrast, in the solution of pH 9.0, longer fibrils are found as shown in Table I.

To study the effects of multivalent ions on the self-assembling process of ionic-complementary peptide, three types of salts with multivalent anions (sodium sulfate, sodium citrate, and sodium phosphate) are used. The hydrolyte equation of SO_4^{2-} is

$$SO_4^{2-} + H_2O \rightleftharpoons HSO_4^- + OH^-. \quad (1)$$

The anions in sodium sulfate solution are almost SO_4^{2-} at all three pHs (pH 4.5, 6.5, and 9.0) by virtue of the low p*K*a of HSO_4^- (1.99). At pH 4.5, no fibrils but amorphous aggregates are observed as shown in Figure 5A. At pH 6.5, only a few short fibrils could be found (Figure 5B) with an average length of 132.9 ± 13.0 nm as listed in Table II. Differently, for the case of pH 9.0, the net negative charges on peptide decrease the effect of divalent anion on self-assembly process and make it possible to form some longer fibrils as shown in Figure 5C. Furthermore, for the cases of all the three pH conditions, it is observed from the CD spectra (shown in Figure 4) that the positions of the negative peaks shift to about 220 nm and that the corresponding amplitudes decrease, indicating an obvious loss of the β-sheet structure. This phenomenon is different from that of the monovalent anions as discussed above. In fact, although small amounts of fibrils are observed by AFM technique, numerous amorphous aggregates are found during the incubation period and their corresponding average particle diameters are >1000 nm as detected by DLS. However, these large amorphous aggregates are too big to be observed by AFM. The divalent anions of SO_4^{2-} largely hinder the formation of fibrils, which is similar to the effect of divalent cations as discussed in previous studies.[18,27] One SO_4^{2-} ion (molecular weight is 96) with two negative charges can easily interact with two positive charges simultaneously like a bridge. This can disturb the ionic-complementary interaction of the peptide, which can destabilize the stability of the amyloid-like fibrils and even induce the formation of amorphous aggregation as shown in Figure 5.

To further elucidate the mechanism of such effect of multivalent anions on the self-assembling process of the peptide EMK16-II, another salt with multivalent anions, namely sodium citrate, is used in this study. The equations of hydrolyzation of citrate radicals are

$$\begin{aligned} &C_6H_5O_7^{3-} + 3H_2O \rightleftharpoons HC_6H_5O_7^{2-} + 2H_2O + OH^- \\ &\rightleftharpoons H_2C_6H_5O_7^- + H_2O + 2OH^- \rightleftharpoons H_3C_6H_5O_7 + 3OH^-, \end{aligned} \quad (2)$$

where two or three kinds of anions can possibly coexist in the solution of sodium citrate at different pH conditions as shown in Table III (based on the p*K*as of citric acid: pK_1 = 3.13, pK_2 = 4.76, pK_3 = 6.40). Such a situation is much more complicated than that of sodium sulfate. As shown in Figures 5D–5F, only a few self-assembling nanofibers of

10970282, 2010, 4, Downloaded from https://onlinelibrary.wiley.com/doi/10.1002/bip.21340 by Universidade do Porto, Wiley Online Library on [02/12/2025]. See the Terms and Conditions (https://onlinelibrary.wiley.com/terms-and-conditions) on Wiley Online Library for rules of use; OA articles are governed by the applicable Creative Commons License

Table I Dimensions of EMK16-II Self-Assembling Nanofibrils in Pure Water, Sodium Chloride, and Sodium Acetate Buffers at Different pHs

	Water	NaCl (pH 4.5)	NaCl (pH 6.5)	NaCl (pH 9.0)	NaAc (pH 4.5)	NaAc (pH 6.50)	NaAc (pH 9.0)
Length (nm)	468.0 ± 24.0	688.3 ± 24.3	880.9 ± 52.0	754.1 ± 26.8	365.9 ± 40.0	522.0 ± 57.4	641.7 ± 39.0
Width (nm)	16.1 ± 1.7	19.1 ± 0.7	22.5 ± 0.6	21.1 ± 0.7	20.5 ± 0.9	17.8 ± 1.1	18.4 ± 1.1
Height (nm)	1.4 ± 0.1	1.7 ± 0.1	1.8 ± 0.1	1.5 ± 0.1	1.8 ± 0.1	2.0 ± 0.1	1.6 ± 0.1

The data were collected from the enlargement of the original images.

EMK16-II are formed in solutions of sodium citrate at different pH conditions, which is similar to the case of sodium sulfate. At pH 4.5, the average length of the fibrils that rarely observed is only 211.4 ± 19.7 nm, which is much shorter than that in pure water and also in monovalent anion solutions as discussed above. At pH 6.5 and 9.0, no fibrils but amorphous aggregates are observed in AFM images (Figures 5E and 5F) because the concentrations of divalent and trivalent anions are extremely high as shown in Table III.

As discussed above, multivalent anions that carry two or three units of negative charge interact with the charged residues simultaneously, especially the positive ones. In addition, another special feature of citrate is the high absorbance in the far UV range. Therefore, we can separate citrate from peptide solutions by gel filtration chromatography. Differently, this specific feature (high absorption in the far UV range) does not exist in most of the other multivalent anions, such as SO_4^{2-}, HPO_4^{2-}, and PO_4^{3-}, which cannot be detected by gel filtration chromatography directly. Thus, we merely took sodium citrate as a typical multivalent salt to verify our results concerning the multivalent anions on the self-assembly of EMK16-II.

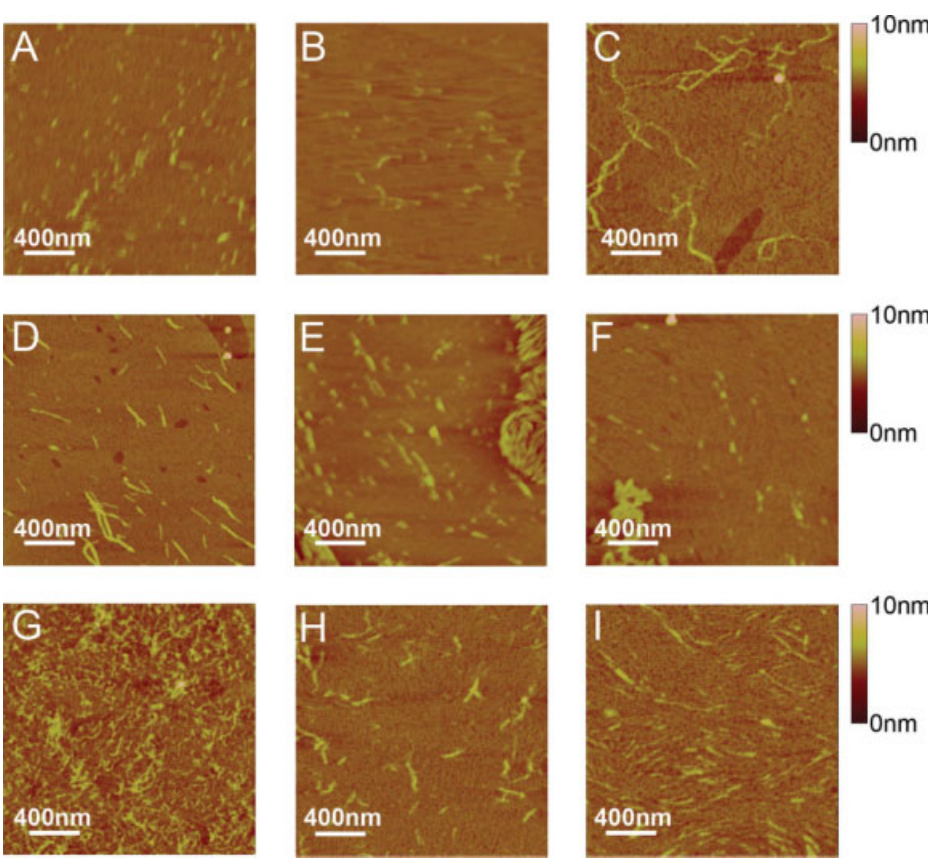

FIGURE 5 AFM images of the self-assembling nanostructures of EMK16-II (0.4 mg/ml) in solutions containing 20 m*M* sodium sulfate buffer at (A) pH 4.5, (B) pH 6.5, and (C) pH 9.0; sodium citrate buffer at (D) pH 4.5, (E) pH 6.5, and (F) pH 9.0; and sodium phosphate buffer at (G) pH 4.5, (H) pH 6.5, and (I) pH 9.0.

10970282, 2010, 4, Downloaded from https://onlinelibrary.wiley.com/doi/10.1002/bip.21340 by Universidade do Porto, Wiley Online Library on [02/12/2025]. See the Terms and Conditions (https://onlinelibrary.wiley.com/terms-and-conditions) on Wiley Online Library for rules of use; OA articles are governed by the applicable Creative Commons License

Table II Dimensions of EMK16-II Self-Assembling Nanofibrils in Sodium Sulfate, Sodium Citrate and Sodium Phosphate Buffers at Different pHs

	Na_2SO_4 (pH 6.5)	Na_2SO_4 (pH 9.0)	Citrate (pH 4.5)	Phosphate (pH 4.5)	Phosphate (pH 6.5)	Phosphate (pH 9.0)
Length (nm)	143.5 ± 15.5	363.3 ± 77.1	211.4 ± 19.7	284.3 ± 14.0	129.4 ± 14.3	233.5 ± 32.1
Width (nm)	15.5 ± 1.8	22.7 ± 1.3	22.0 ± 0.9	21.3 ± 1.0	27.0 ± 1.1	29.4 ± 1.4
Height (nm)	1.7 ± 0.1	1.4 ± 0.1	1.5 ± 0.1	1.4 ± 0.1	1.6 ± 0.1	1.6 ± 0.1

The data were collected from the enlargement of the original images.

All samples before injection are filtered through a 450-nm filter. As shown in Figure 6, two distinctive peaks (solid line), occurring at 2.0 min and 4.3 min, correspond to the filtrated productions of EMK16-II (oligomer, particle diameter <450 nm) and the citrate anions, respectively. After 24-h incubation, the chromatographic peak of EMK16-II (dashed line) almost disappears because the large aggregates of EMK16-II (mean aggregation diameter >1000 nm, DLS) cannot get through the 450-nm filter. For the case of the chromatographic peak of citrate, there is an obvious decrease (about 25%) in the peak area, which implies this part of citrate anions are excluded by the filter with EMK16-II aggregates. These disappeared anions must stay inside the amorphous aggregates and interact with different positive-charged groups like bridges. Bridge effect is extremely important to the formation of amorphous aggregates of the peptide EMK16-II. This is because that one bridge can connect with any two or more positive charged groups (i.e., the NH_3^+ in lysine side chain), which can make the residues with the same charge be closer between peptide molecules and disturb the original ionic-complementary interaction. The repulsive interaction between the residues can further interfere with the formation of intermolecular sequential hydrogen bonds that control the fibrillar growth. Therefore, the hydrophobic interaction becomes the most important driving force and makes the peptide self-assemble into amorphous aggregates. This can well elucidate the effects of multivalent anions on the self-assembling process of ionic-complementary peptides. It is noted that the monovalent and multivalent anions coexist in the peptide solution as listed in Table III. The effect of multivalent anion with sufficient concentration may be dominant in preventing the formation of ordered fibrils. In fact, the puzzles in previous studies why divalent cations are not suitable for the formation of ordered nanostructures of the ionic-complimentary peptides can also be elucidated by such a mechanism.[9,26,40] However, the detailed effect of the anions with double or triple valences cannot be discriminated, which requires further studies.

Sodium phosphate is also applied in this work to investigate all the phenomena discussed above, because the anions in solution can be modulated from monovalent to multivalent through adjusting the pH values of solutions. As a polybasic acid radical, the PO_4^{3-} is hydrolyzed with water as follows:

$$\begin{aligned} &PO_4^{3-} + 3H_2O \rightleftharpoons HPO_4^{2-} + 2H_2O + OH^- \\ &\rightleftharpoons H_2PO_4^- + H_2O + 2OH^- \rightleftharpoons H_3PO_4 + 3OH^-. \end{aligned} \quad (3)$$

In Table IV, the concentrations of the three kinds of anions ($H_2PO_4^-$, HPO_4^{2-}, and PO_4^{3-}) in solutions are listed according to the values of p*K*a of the phosphoric acid ($pK_1 = 2.13$, $pK_2 = 7.20$, $pK_3 = 12.36$). At pH 4.5, about 99.4% phosphate radicals exist in the monovalent form ($H_2PO_4^-$). Similar to the effects of other monovalent anions mentioned above, plenty of nanofibrils are also found without large amorphous aggregates as shown in Figure 5G. In addition, the corresponding CD spectrum of sodium phosphate at pH 4.5 (shown in Figure 4A) indicates that the well ordered fibrils are composed of the β-sheet structures according to other monovalent anions discussed above. However, the length of fibrils is shorter than that in pure water because of the steric effect of $H_2PO_4^-$, which is also similar to the case of the sodium acetate at acidic condition. As listed in Table IV, plenty of HPO_4^{2-} radicals exist in the solutions at pH 6.5

Table III The Concentrations of Citric Acid and Other Different Anions ($H_2C_6H_5O_7^-$, $HC_6H_5O_7^{2-}$, and $C_6H_5O_7^{3-}$) in Sodium Citrate Solutions due to the Hydrolyzation at Different pHs

	$[H_3C_6H_5O_7]$ (m*M*)	$[H_2C_6H_5O_7^-]$ (m*M*)	$[HC_6H_5O_7^{2-}]$ (m*M*)	$[C_6H_5O_7^{3-}]$ (m*M*)	Sum (m*M*)
pH 4.5	0.53	12.50	6.88	0.09	20.00
pH 6.5	0	0.16	8.84	11.00	20.00
pH 9.0	0	0	0	20.00	20.00

10970282, 2010, 4, Downloaded from https://onlinelibrary.wiley.com/doi/10.1002/bip.21340 by Universidade do Porto, Wiley Online Library on [02/12/2025]. See the Terms and Conditions (https://onlinelibrary.wiley.com/terms-and-conditions) on Wiley Online Library for rules of use; OA articles are governed by the applicable Creative Commons License

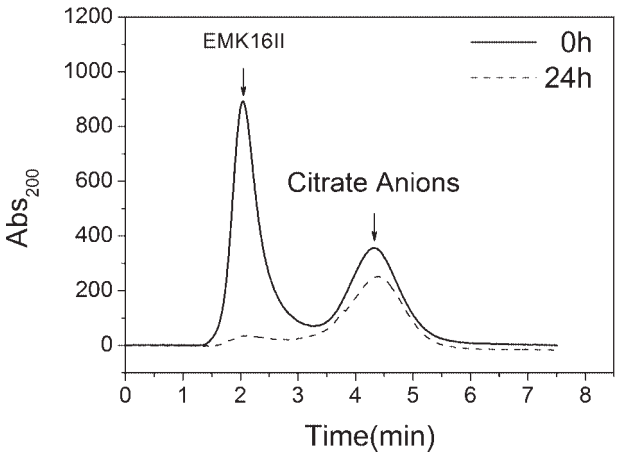

FIGURE 6 Gel filtration chromatography of solution containing 0.4 mg/ml EMK16-II in the presence of 20 m*M* sodium citrate at pH 6.5 with no incubation (solid line) and 24-h incubation (dashed line). The peak at 2.0 min corresponds to EMK16-II (monomer or oligomer), and the peak at 4.3 min corresponds to the citrate anions, whose molecular weight are much lower than that of the peptide. All samples were filtered through a 450-nm filter just before use.

and 9.0. Therefore, only a few short fibrils are found as shown in Figures 4H and 4I because of the bridge effect of HPO_4^{2-} or PO_4^{3-} among the positive-charged side chains. At the same time, large amorphous aggregates are also observed (mean aggregates diameter >1000 nm, DLS), and the reason has been discussed above just similar to that of other multivalent anions. Because the distance between two nearest lysine residues of the same peptide molecule is large and sizes of the anions, e.g., SO_4^{2-} and HPO_4^{2-}, are quite small, one anion could not interact with more than one lysine residues simultaneously. The size of the citrate radical is more or less the same as the distance between two nearest lysine residues. Most of the citrate anions carry three net negative charges on each radical at neutral and basic pHs. Although it is presumable that two negative charges can interact with the two lysine residues of the same peptide molecule, there is still one superfluous net charge available to interact with lysine residue of another peptide molecule. It is worthy to note that the intrinsic features of ions, such as their sizes, charge densities, etc., are also very important in the folding and stability of proteins or peptides as well as their self-assembling process.[18,49–51] However, the effects induced by different valences of the ions are more prominent than those resulted from the features of ions with the same valence. The latter is not investigated in this work in detail.

On the basis of these results, we present a proposed cartoon model for the formation process of fibrils from its soluble peptides as shown in Figure 7. In the fibril growth direction, electrostatic interactions play a vital role in forming β-sheet fibrils (from monomer to dimmer, oligomer, nuclei, and fibrils) because of the ionic-complementary behavior, thus it can easily be affected by the salt with different valences of anions. At the same time, the hydrogen bonds also perform an important role in maintaining the length of the fibrils. In addition, two monolayer β-sheet aggregates can stack together because of the hydrophobic interaction. It is noted that the strong hydrophobic interaction can also tend to aggregate to hydrophobic cluster, when the ionic-complementary behavior is destroyed by the addition of multivalent anions. This can destroy the formation of ordered fibrils and further induce the formation of amorphous aggregates.

MATERIALS AND METHODS

Fmoc-Lys(Boc)-Wang resin (100–200 mesh, subst.: 0.66 mmol/g), Fmoc-Met-OH, Fmoc-Glu (OtBu)-OH, Fmoc-Lys (Boc)-OH, and *O*-benzotriazole-*N*,*N*,*N*,*N*-tetramethyl-uroniumhexafluoro-phosphate (HBTU) were purchased from NovaBiochem (Merck Biosciences AG). GC grade *N*,*N*-dimethylformamide, 4-methylmorpholine, trifluoroacetic acid, and piperidine 99% were ordered from Merck Schuchardt. Triisopropylsilane 99% was obtained from Aldrich. Dichloromethane (HPLC/SPECTRO) and acetonitrile (HPLC/SPECTRO) were purchased from TEDIA. DTT was ordered from Amresco. Other chemicals were obtained from SCRC.

Ionic-Complementary Peptide: EMK16-II

We chose a new self-assembling oligopeptide, EMK16II (MEM EMKMKMEMEMKMK, where M corresponds to methionine, E to glutamic acid, and K to lysine), which was named by the same nominating rule[22] of EAK16-II. EMK16-II contained three kinds of amino acids (Met, Glu, and Lys), which constituted a 16-amino acid long sequence. The hydrophobic residue Met and hydrophilic residues Glu and Lys were lined in a regularly organized sequence, which led to particular amphiphilic property. In addition, these

Table IV The Concentrations of Phosphoric Acid and Other Different Anions ($H_2PO_4^-$, HPO_4^{2-}, and PO_4^{3-}) in Sodium Phosphate Solutions due to the Hydrolyzation at Different pHs

	$[H_3PO_4]$ (m*M*)	$[H_2PO_4^-]$ (m*M*)	$[HPO_4^{2-}]$ (m*M*)	$[PO_4^{3-}]$ (m*M*)	Sum (m*M*)
pH 4.5	0.08	19.88	0.04	0	20.00
pH 6.5	0	16.67	3.33	0	20.00
pH 9.0	0	0.32	19.67	0.01	20.00

10970282, 2010, 4, Downloaded from https://onlinelibrary.wiley.com/doi/10.1002/bip.21340 by Universidade do Porto, Wiley Online Library on [02/12/2025]. See the Terms and Conditions (https://onlinelibrary.wiley.com/terms-and-conditions) on Wiley Online Library for rules of use; OA articles are governed by the applicable Creative Commons License

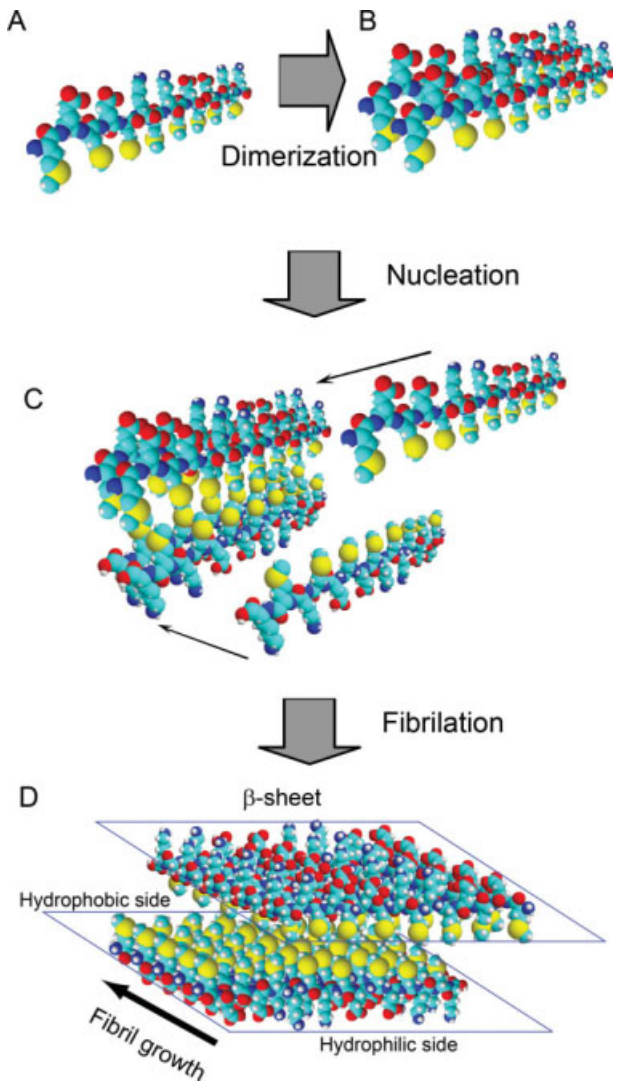

FIGURE 7 A proposed cartoon model of the self-assembling process of EMK16-II from soluble peptide molecules (A) to dimers (B), nuclei (C), and fibrils (D).

hydrophilic residues formed alternating negative and positive charges along the sequence: − − + + − − + +. This ionic-complementary feature and the hydrophobic interactions made the adjacent peptide molecules interact, which favored the formation of the well-ordered β-sheet structures.[52] It is noted that the methionine in peptides can easily become oxidized, and as a result, the formation of aggregates will be greatly influenced as mentioned in previous studies.[53,54] However, because the synthesized condition and the strong self-assembling ability with hydrophobic residues packing together, the oxidation of methionine to sulfoxide or sulfone in this work is almost avoided. It is found that even in pure water without reducing agent, there is not any above-mentioned oxidized product by mass spectroscopy (data not shown).

Peptide Synthesis

EMK16-II was synthesized using Fmoc chemistry on a Symphony Quartet peptide synthesizer (Protein Technologies, USA).

Purification and Desalting

Peptide purification was performed via reverse-phase chromatography on a AKTABasic pH/C 10 ml System (Amersham Biosciences) equipped with a Source 5RPC ST4.6/150 column (Amersham Biosciences; Polystyrene matrix, 5 μm particle size, 4.6 × 150 mm).

Peptide desalting was performed via gel filtration chromatography on AKTABasic with a Hitrap Desalting column (Sephadex G-25, 5 ml). The peptide was eluted from the column with pure water at 2.0 ml/min.

Sample Preparation

Lyophilized peptide powder was dissolved in ultrapure water (18.2 MO; Millipore Milli-Q system) or buffer solutions (20 m*M*) to get a final concentration of 0.4 mg/ml. The concentrations of all the samples used for AFM imaging, CD measurements, and peptide gel filtration chromatography were 0.4 mg/ml unless specified. The p*I* of EMK16-II was calculated to be about 6 (http://www.expasy.ch/tools/pi_tool.html). Three pH points, from acid to basic condition, were discussed in this study. Unless noted for special purpose, the solutions were stirred at room temperature for hours before AFM imaging and CD measurements.

AFM

About 5 μl of the peptide solution was placed on the surface of a newly peeled mica surface. Each sample was placed on the mica for 10 minutes and then rinsed with 100 μl of pure water to remove unattached peptides and salts. Then, the peptide sample on the mica surface was air dried, and images were acquired immediately.

The images were obtained by scanning the mica surface at room temperature by a Nanoscope IIIa (Digital Instruments, USA) operating in tapping mode (conditions: scan rate, 0.8 Hz; resonant frequency range of AFM tips, 204–497 kHz; tip radius, 5 nm; number of pixels, 512 × 512.). A scanner with a maximum scan size of 10 μm was used. Data sets were subjected to a first-order flattening. To obtain typical images in each case, different samples and three regions in the entire surface were scanned.

The AFM images were enlarged to perform the quantified measurement of dimensions. The fibrils length was calculated by the ImageJ software. The width and height of the fibrils were measured by NanoScope software. All the statistics were acquired by measuring >50 random fibrils manually.

For the dimensions of the assemblies, it was found that the widths were broadened because of the convolution effects arising from the finite size of the AFM tip.[3,55–57] Thus, the observed values for the dimensions had to be corrected. For a spherical sample with a radius of R_m, the observed width of the sample has a relationship, $W_{obs} = 4(R_t R_m)^{1/2}$, where R_t is the radius of the AFM tip.[58–60] When the sample is assumed to be a sheet, the real width of the sheet can be obtained by the following equation, $W = W_{obs} - 2(2R_t H - H^2)^{1/2}$, where H is the observed height.[25]

Circular Dichroism

CD spectra were measured using a JASCO J-810 CD spectropolarimeter (Jasco, Japan). All the solutions had the same buffer concentration (20 m*M*) with different pHs (from 4.5 to 9.0). With a 1-mm path length quartz cell, a wavelength scan was done from 250

10970282, 2010, 4, Downloaded from https://onlinelibrary.wiley.com/doi/10.1002/bip.21340 by Universidade do Porto, Wiley Online Library on [02/12/2025]. See the Terms and Conditions (https://onlinelibrary.wiley.com/terms-and-conditions) on Wiley Online Library for rules of use; OA articles are governed by the applicable Creative Commons License

to 190 nm at room temperature. All spectra were baseline corrected before analysis.

LS and DLS

The LS experiments were performed on a JASCO FP-6500 spectrofluorometer fluorescence system (Jasco) with a xenon lamp as the light source. Samples were irradiated at 314 nm,[25] and scattered light was monitored at 314 nm for 10 min with a data pitch of 0.2 s. Excitation and emission slits widths were set to 3 and 1 nm, respectively. An average value of 3000 data points was calculated for each spectrum. All samples were tested in 1-h intervals initially and then once a day over a period of >3 weeks.

All DLS experiments were performed on a BI-200SM instrument (Brookhaven, USA) at room temperature. LS intensity at a 90° angle was collected using a 3-min acquisition time. Particle diffusion coefficients were calculated from light intensity data and converted to radius with the Stokes-Einstein equation.

CONCLUSIONS

In this work, effects of the important hydrophobic and electrostatic interactions on the self-assembling process of an ionic-complementary peptide EMK16-II are studied. It is found that strong hydrophobicity of the peptide promotes the aggregation in pure water even at very low concentrations, which yields a much lower CAC than that of EAK16-II, a previously reported peptide.[25] The effects of anions with different valences on the electrostatic interaction are investigated using AFM imaging, CD spectrum, LS, DLS, and chromatography. The formation of nanofibrils is observed to be facilitated by the monovalent ions in solutions of sodium chloride and sodium acetate because of their screening effect on the net charges of the peptide molecules. In addition, steric effect of Cl^- of smaller size is less effective than that of Ac^- of larger size. When the peptide solutions are incubated with multivalent anions, such as SO_4^{2-}, $C_6H_5O_7^{3-}$, and HPO_4^{2-}, only small amounts of fibrils but plenty of large amorphous aggregates are found, which is also observed for EAK16-II. Most importantly, the multivalent citrate anions are found to reside and interact tightly within the amorphous aggregates by gel filtration chromatography, which is perhaps similar as the other multivalent anions. One multivalent anion can interact with two or more positively charged residues like a bridge, which can disturb the specific ionic-complementary characteristic of EMK16-II and inhibits the fibril growth by affecting the formation of well-ordered hydrogen bonds. In addition, the formation of large amorphous aggregates results mainly from the hydrophobic interactions that become more dominant. The puzzles in previous studies why divalent cations are the inhibitors of the formation of ordered nanostructure of the ionic-complimentary peptides are elucidated by the effect of the salt bridge.

The results of our study present an interpretation for the effects of hydrophobic and electrostatic interactions in the self-assembling process of the ionic-complementary peptides. This provides a clue for the control on the self-assembling of the nanostructures, for example, by changing the hydrophobicity of the peptide, adding different types of anions, or adjusting pH condition of the solutions. These methods can be easily realized to modulate the self-assembled nanostructures of the ionic-complimentary peptides, which have significant implications beyond supramolecular chemistry and biological materials, i.e., drug delivery, wound healing, and tissue engineering.[22,39] Furthermore, understanding such a self-assembling process of the ionic-complimentary peptides is also helpful for investigating the underlying mechanism of the related protein folding and aggregation.[61–69] Finally, it is important to perform studies with high resolution in exploring the detailed effect of multivalent anions on the self-assembly of peptides.

REFERENCES

1. Gazit, E.; Tendler, S. J. B. Curr Opin Chem Biol 2006, 10, 385–386.
2. Carrell, R. W.; Lomas, D. A. Lancet 1997, 350, 134–138.
3. Chamberlain, A. K.; MacPhee, C. E.; Zurdo, J.; Morozova-Roche, L. A.; Hill, H. A. O.; Dobson, C. M.; Davis, J. J. Biophys J 2000, 79, 3282–3293.
4. Kelly, J. W.; Lansbury, P. T. Amyloid 1994, 1, 186–205.
5. Pan, K. M.; Baldwin, M.; Nguyen, J.; Gasset, M.; Serban, A.; Groth, D.; Mehlhorn, I.; Huang, Z. W.; Fletterick, R. J.; Cohen, F. E.; Prusiner, S. B. Proc Natl Acad Sci USA 1993, 90, 10962–10966.
6. Fraser, P. E.; McLachlan, D. R.; Surewicz, W. K.; Mizzen, C. A.; Snow, A. D.; Nguyen, J. T.; Kirschner, D. A. J Mol Biol 1994, 244, 64–73.
7. Hong, Y. S.; Legge, R. L.; Zhang, S.; Chen, P. Biomacromolecules 2003, 4, 1433–1442.
8. Caplan, M. R.; Lauffenburger, D. A. Ind Eng Chem Res 2002, 41, 403–412.
9. Chen, P. Colloids Surf A 2005, 261, 3–24.
10. Holmes, T. C.; de Lacalle, S.; Su, X.; Liu, G. S.; Rich, A.; Zhang, S. G. Proc Natl Acad Sci USA 2000, 97, 6728–6733.
11. Nowak, A. P.; Breedveld, V.; Pakstis, L.; Ozbas, B.; Pine, D. J.; Pochan, D.; Deming, T. J. Nature 2002, 417, 424–428.
12. Zhang, S. G.; Marini, D. M.; Hwang, W.; Santoso, S. Curr Opin Chem Biol 2002, 6, 865–871.
13. Hartgerink, J. D.; Beniash, E.; Stupp, S. I. Science 2001, 294, 1684–1688.
14. Vauthey, S.; Santoso, S.; Gong, H. Y.; Watson, N.; Zhang, S. G. Proc Natl Acad Sci USA 2002, 99, 5355–5360.
15. Whaley, S. R.; English, D. S.; Hu, E. L.; Barbara, P. F.; Belcher, A. M. Nature 2000, 405, 665–668.
16. Lee, S. W.; Mao, C. B.; Flynn, C. E.; Belcher, A. M. Science 2002, 296, 892–895.
17. Zhang, S. G. Biotechnol Adv 2002, 20, 321–339.

10970282, 2010, 4, Downloaded from https://onlinelibrary.wiley.com/doi/10.1002/bip.21340 by Universidade do Porto, Wiley Online Library on [02/12/2025]. See the Terms and Conditions (https://onlinelibrary.wiley.com/terms-and-conditions) on Wiley Online Library for rules of use; OA articles are governed by the applicable Creative Commons License

18. Zhang, S. G.; Holmes, T.; Lockshin, C.; Rich, A. Proc Natl Acad Sci USA 1993, 90, 3334–3338.
19. Zhang, S. G.; Holmes, T. C.; Dipersio, C. M.; Hynes, R. O.; Su, X.; Rich, A. Biomaterials 1995, 16, 1385–1393.
20. Altman, M.; Lee, P.; Rich, A.; Zhang, S. G. Protein Sci 2000, 9, 1095–1105.
21. Zhang, S. G.; Lockshin, C.; Cook, R.; Rich, A. Biopolymers 1994, 34, 663–672.
22. Zhang, S. G.; Altman, M. React Funct Polym 1999, 41, 91–102.
23. Jun, S.; Hong, Y.; Imamura, H.; Ha, B. Y.; Bechhoefer, J.; Chen, P. Biophys J 2004, 87, 1249–1259.
24. Keyes-Baig, C.; Duhamel, J.; Fung, S. Y.; Bezaire, J.; Chen, P. J Am Chem Soc 2004, 126, 7522–7532.
25. Fung, S. Y.; Keyes, C.; Duhamel, J.; Chen, P. Biophys J 2003, 85, 537–548.
26. Yang, H.; Pritzker, M.; Fung, S. Y.; Sheng, Y.; Wang, W.; Chen, P. Langmuir 2006, 22, 8553–8562.
27. Hong, Y. S.; Lau, L. S.; Legge, R. L.; Chen, P. J Adhes 2004, 80, 913–931.
28. Hartgerink, J. D.; Beniash, E.; Stupp, S. I. Proc Natl Acad Sci USA 2002, 99, 5133–5138.
29. Zhao, Y.; Yokoi, H.; Tanaka, M.; Kinoshita, T.; Tan, T. W. Biomacromolecules 2008, 9, 1511–1518.
30. Chiti, F.; Webster, P.; Taddei, N.; Clark, A.; Stefani, M.; Ramponi, G.; Dobson, C. M. Proc Natl Acad Sci USA 1999, 96, 3590–3594.
31. Greenfie, N.; Fasman, G. D. Biochemistry 1969, 8, 4108–4116.
32. Barrow, C. J.; Zagorski, M. G. Science 1991, 253, 179–182.
33. Aggeli, A.; Bell, M.; Carrick, L. M.; Fishwick, C. W. G.; Harding, R.; Mawer, P. J.; Radford, S. E.; Strong, A. E.; Boden, N. J Am Chem Soc 2003, 125, 9619–9628.
34. Nandi, P. K.; Robinson, D. R. J Am Chem Soc 1972, 94, 1299–1308.
35. Hong, Y.; Pritzker, M. D.; Legge, R. L.; Chen, P. Colloids Surf B 2005, 46, 152–161.
36. Zou, D. W.; Tie, Z. X.; Qin, M.; Lu, C. M.; Wang, W. Chin Phys Lett 2009, 26.
37. de la Paz, M. L.; Goldie, K.; Zurdo, J.; Lacroix, E.; Dobson, C. M.; Hoenger, A.; Serrano, L. Proc Natl Acad Sci USA 2002, 99, 16052–16057.
38. Yu, Y.; Monera, O. D.; Hodges, R. S.; Privalov, P. L. J Mol Biol 1996, 255, 367–372.
39. Caplan, M. R.; Moore, P. N.; Zhang, S. G.; Kamm, R. D.; Lauffenburger, D. A. Biomacromolecules 2000, 1, 627–631.
40. Dahlgren, P. R.; Lyubchenko, Y. L. Biochemistry 2002, 41, 11372–11378.
41. http://www.acdlabs.com.
42. Yokoi, H.; Kinoshita, T.; Zhang, S. G. Proc Natl Acad Sci USA 2005, 102, 8414–8419.
43. Yang, H.; Fung, S.-Y.; Pritzker, M.; Chen, P. PLoS One 2007, 2, e1325–e1325.
44. Chen, Y. H.; Yang, J. T.; Chau, K. H. Biochemistry 1974, 13, 3350–3359.
45. Sonnichsen, F. D.; Vaneyk, J. E.; Hodges, R. S.; Sykes, B. D. Biochemistry 1992, 31, 8790–8798.
46. Klunk, W. E.; Jacob, R. F.; Mason, R. P. Anal Biochem 1999, 266, 66–76.
47. Yang, H.; Fung, S. Y.; Pritzker, M.; Chen, P. J Am Chem Soc 2007, 129, 12200–12210.
48. Kad, N. M.; Myers, S. L.; Smith, D. P.; Smith, D. A.; Radford, S. E.; Thomson, N. H. J Mol Biol 2003, 330, 785–797.
49. Zhou, N. E.; Kay, C. M.; Hodges, R. S. J Mol Biol 1994, 237, 500–512.
50. Hoshino, M.; Yumoto, N.; Yoshikawa, S.; Goto, Y. Protein Sci 1997, 6, 1396–1404.
51. Jelesarov, I.; Durr, E.; Thomas, R. M.; Bosshard, H. R. Biochemistry 1998, 37, 7539–7550.
52. Brack, A.; Orgel, L. E. Nature 1975, 256, 383–387.
53. Johansson, A. S.; Bergquist, J.; Volbracht, C.; Paivio, A.; Leist, M.; Lannfelt, L.; Westlind-Danielsson, A. Neuroreport 2007, 18, 559–563.
54. Choi, J.; Sullards, M. C.; Olzmann, J. A.; Rees, H. D.; Weintraub, S. T.; Bostwick, D. E.; Gearing, M.; Levey, A. I.; Chin, L. S.; Li, L. J Biol Chem 2006, 281, 10816–10824.
55. Forbes, J. G.; Jin, A. J.; Wang, K. Langmuir 2001, 17, 3067–3075.
56. Goldsbury, C.; Kistler, J.; Aebi, U.; Arvinte, T.; Cooper, G. J. S. J Mol Biol 1999, 285, 33–39.
57. Ionescu-Zanetti, C.; Khurana, R.; Gillespie, J. R.; Petrick, J. S.; Trabachino, L. C.; Minert, L. J.; Carter, S. A.; Fink, A. L. Proc Natl Acad Sci USA 1999, 96, 13175–13179.
58. Gale, M.; Pollanen, M. S.; Markiewicz, P.; Goh, M. C. Biophys J 1995, 68, 2124–2128.
59. Markiewicz, P.; Goh, M. C. Langmuir 1994, 10, 5–7.
60. Vesenka, J.; Guthold, M.; Tang, C. L.; Keller, D.; Delaine, E.; Bustamante, C. Ultramicroscopy 1992, 42, 1243–1249.
61. van Raaij, M. J.; Mitraki, A.; Lavigne, G.; Cusack, S. Nature 1999, 401, 935–938.
62. Kelly, J. W.; Balch, W. E. J Cell Biol 2003, 161, 461–462.
63. Dobson, C. M. Trends Biochem Sci 1999, 24, 329–332.
64. Krebs, M. R. H.; Wilkins, D. K.; Chung, E. W.; Pitkeathly, M. C.; Chamberlain, A. K.; Zurdo, J.; Robinson, C. V.; Dobson, C. M. J Mol Biol 2000, 300, 541–549.
65. Rochet, J. C.; Lansbury, P. T. Curr Opin Struct Biol 2000, 10, 60–68.
66. Polymeropoulos, M. H. Ann Neurol 1998, 44, S63–S64.
67. Lee, S.; Eisenberg, D. Nat Struct Biol 2003, 10, 725–730.
68. Scheibel, T.; Parthasarathy, R.; Sawicki, G.; Lin, X. M.; Jaeger, H.; Lindquist, S. L. Proc Natl Acad Sci USA 2003, 100, 4527–4532.
69. Inoue, Y.; Kishimoto, A.; Hirao, J.; Yoshida, M.; Taguchi, H. J Biol Chem 2001, 276, 35227–35230.

Reviewing Editor: Eric J. Toone

10970282, 2010, 4, Downloaded from https://onlinelibrary.wiley.com/doi/10.1002/bip.21340 by Universidade do Porto, Wiley Online Library on [02/12/2025]. See the Terms and Conditions (https://onlinelibrary.wiley.com/terms-and-conditions) on Wiley Online Library for rules of use; OA articles are governed by the applicable Creative Commons License